JOURNAL OF VIROLOGY, Feb. 2000, p. 1919–1930 Vol. 74, No. 4
0022-538X/00/$04.00+0

Cellular Uptake and Infection by Canine Parvovirus Involves Rapid Dynamin-Regulated Clathrin-Mediated Endocytosis, Followed by Slower Intracellular Trafficking

JOHN S. L. PARKER AND COLIN R. PARRISH*

James A. Baker Institute for Animal Health, College of Veterinary Medicine, Cornell University, Ithaca, New York 14853

Received 11 May 1999/Accepted 18 November 1999

Canine parvovirus (CPV) is a small, nonenveloped virus that is a host range variant of a virus which infected cats and changes in the capsid protein control the ability of the virus to infect canine cells. We used a variety of approaches to define the early stages of cell entry by CPV. Electron microscopy showed that virus particles concentrated within clathrin-coated pits and vesicles early in the uptake process and that the infecting particles were rapidly removed from the cell surface. Overexpression of a dominant interfering mutant of dynamin in the cells altered the trafficking of capsid-containing vesicles. There was a 40% decrease in the number of CPV-infected cells in mutant dynamin-expressing cells, as well as a ~40% decrease in the number of cells in S phase of the cell cycle, which is required for virus replication. However, there was also up to 10-fold more binding of CPV to the surface of mutant dynamin-expressing cells than there was to uninduced cells, suggesting an increased receptor retention on the cell surface. In contrast, there was little difference in virus binding, virus infection rate, or cell cycle distribution between induced and uninduced cells expressing wild-type dynamin. CPV particles colocalized with transferrin in perinuclear endosomes but not with fluorescein isothiocyanate-dextran, a marker for fluid-phase endocytosis. Cells treated with nanomolar concentrations of bafilomycin A1 were largely resistant to infection when the drug was added either 30 min before or 90 min after inoculation, suggesting that there was a lag between virus entering the cell by clathrin-mediated endocytosis and escape of the virus from the endosome. High concentrations of CPV particles did not permeabilize canine A72 or mink lung cells to α-sarcin, but canine adenovirus type 1 particles permeabilized both cell lines. These data suggest that the CPV entry and infection pathway is complex and involves multiple vesicular components.

The early steps of virus entry into cells involve attachment to the cell surface, followed by penetration of the virion or its components into the cytoplasm through the plasma membrane or the membrane of an endocytic vesicle. For many enveloped and nonenveloped viruses such as influenza virus, Semliki Forest virus, vesicular stomatitis virus, adenovirus, and reovirus, endocytic uptake is required for infection (36, 54, 57, 79). Other viruses such as herpesviruses, rotavirus, poliovirus, and some retroviruses may enter the cytoplasm by penetrating or fusing directly to the plasma membrane after binding their appropriate receptors (41, 50, 61, 75).

The general endocytic mechanisms by which ligands including viruses can be taken into the cell are clathrin-mediated endocytosis, uptake via caveolae, macropinocytosis, a poorly characterized caveolin- and clathrin-independent pathway, and phagocytosis (55). Electron microscopic studies show that many viruses bind to coated regions of the plasma membrane and are found in coated vesicles, indicating that they are taken into cells by clathrin-mediated endocytosis, e.g., adenovirus, minute virus of mice (MVM), and influenza virus (46, 53, 60). In contrast, entry and infection of cells by simian virus 40 (SV40) has been shown to occur via caveolae (2).

Canine parvovirus (CPV) is a variant of a feline parvovirus which gained the ability to infect dog cells and dogs through a small number of sequence changes in its capsid coat protein (76). CPV most likely enters and infects cells by an endocytic route as agents which prevent endosome trafficking or acidification block virus infection or replication (8, 81). The uptake of CPV from the plasma membrane has been suggested to occur via a non-clathrin-dependent endocytic pathway on the basis of electron microscopic examination of cells after 15 min of incubation at 37°C (8). However, coated pits and vesicles are short lived, and coated vesicles containing viral particles may rapidly lose their coats. A study of adenovirus entry found the majority of particles within noncoated vesicles, with only a minority of virions bound to coated pits (60). In addition, uptake of the autonomous parvovirus MVM from the plasma membrane occurs within coated vesicles (46). Therefore, it remains possible that CPV infects cells by clathrin-mediated endocytosis.

To initiate infection, CPV must bind to the cells, pass through an endocytic pathway, and eventually deliver its single-stranded DNA genome to the nucleus for replication. CPV has been reported to bind to the basolateral surface of polarized MDCK epithelial cells to a sixfold-greater degree than to the apical surface (7). However, as those cells were not permissive to CPV, the role of that binding in infection is unknown. About 10^5 high-affinity receptors are reported to be present on the surface of canine A72 cells, and maximal binding of CPV is reached after approximately 1 h of incubation at 4°C (7, 8).

The receptor used for CPV infection has not yet been defined. CPV binds sialic acid, and although sialidase treatment of cells reduces virus binding by ~30%, that does not prevent CPV infection, and a non-sialic acid binding mutant of CPV is highly infectious for cells (5). CPV binds 42- and 116-kDa

* Corresponding author. Mailing address: James A. Baker Institute for Animal Health, College of Veterinary Medicine, Cornell University, Ithaca, NY 14853. Phone: (607) 256-5649. Fax: (607) 256-5608. E-mail: crp3@cornell.edu.

proteins when cellular protein blots are probed with virus, and it also binds to a glycophosphotidylinositol-linked protein on feline lymphoid cells, although none of these molecules have been confirmed as the receptor used during infection (6, 9). Among other parvoviruses, sialidase treatment of cells blocks infection by MVM, and the receptor for human B19 parvovirus on erythroid cells is globoside, the erythrocyte P antigen (12, 19). Aleutian mink disease parvovirus binds a 67-kDa protein on the surface of Crandell feline kidney cells, and a polyclonal serum against this protein inhibits infection (31). Adeno-associated virus type 2 binds to heparan sulfate, and it also binds to a 150-kDa cell membrane-associated glycoprotein in overlay blots (56, 73), while human fibroblast growth factor and/or the αVβ5 integrin are coreceptors for adeno-associated virus type 2 entry and infection (65, 72).

Ligands that are taken into cells by receptor-mediated endocytosis are trafficked to early sorting endosomes where the low-pH environment causes many ligands to dissociate from their receptors. Receptor-dissociated ligands are rapidly trafficked to late endosomes and then to lysosomes, where they are degraded (55, 68). Specific signals on the cytoplasmic tail of some receptors may cause them to be sorted and returned to the plasma membrane for reuse, while in other cases both the receptor and ligand are targeted to the late endosome/lysosome for degradation (55). The fate of internalized ligands and receptors is complex, and other pathways exist which target receptors and receptor-bound ligands to a perinuclear recycling endosomal compartment and in some cases to the Golgi network (34, 49).

The specific role of endocytosis in CPV infection and the details of the pathways used are still not well understood. CPV particles taken into cells appear to be trafficked to a perinuclear vesicular compartment, and capsid proteins are largely intact for several hours after uptake (81, 83). CPV infection of A72 cells can be inhibited with the microtubule-depolymerizing agent nocodazole or by incubation at 18°C (81). Trafficking between the early endosome and the late endosome or recycling endosome is microtubule dependent and inhibited by incubation at <20°C (33, 66), which may indicate that CPV infection requires that the capsid be trafficked beyond the early endosome. It is also possible that microtubules are required to transport the capsid within the cytoplasm, similar to what has been shown for herpesvirus and adenovirus (70, 74).

Many viruses require exposure to an acidic pH during infectious entry into cells (51). For example, influenza virus and Semliki Forest virus require exposure to pH of less than 6.0 in the endosome to cause their glycoprotein spike complexes to undergo conformational changes needed for fusion of the viral envelope with cellular membranes (13, 28, 44), and treating cells with agents which disrupt endosomal acidification processes blocks infection (43, 53). Nonenveloped viruses affected by drug treatments which prevent endosomal acidification include adenovirus type 2 (79), rhinoviruses (63), reovirus (52, 57), and CPV (8), while SV40 (42), poliovirus (61), and hepatitis B virus (68) are not affected by such treatments. However, as well as their direct effects on pH, treatments that prevent acidification of endosomes can also inhibit endosomal trafficking within the cell. Infection by some pH-dependent viruses may therefore be inhibited by these agents because of indirect effects of the treatments on endosomal protease activation or on endosomal trafficking of the viral particle (4, 10, 17).

CPV infection is blocked in cells treated with NH_4Cl or chloroquine, indicating that acidification of endosomes may be required (8). However, the capsid appears not to be directly affected by exposure to low pH. The structures of CPV and feline parvovirus empty capsids at pH 5.5 or 6.2 determined by X-ray crystallography show relatively small changes compared to the structures determined at pH 7.5 (A. Simpson, C. R. Parrish, and M. G. Rossmann, unpublished data), and there is little difference in susceptibility of the capsid to proteases at pH 5.5 and 7.5 (83).

Overexpression of mutants of dynamin I defective in GTP binding in a variety of different cells and organisms leads to inhibition of clathrin-mediated endocytosis (16, 18, 23–25, 78). Expression of the dynamin K44A mutant in HeLa cells reduced or prevented the infectious entry of adenovirus, Semliki Forest virus, Sindbis virus, or human rhinovirus 14, indicating that uptake of these viruses requires an active clathrin-mediated endocytic pathway (27, 82). Dynamin is a large 100-kDa GTPase required for scission of clathrin-coated vesicles budding from the plasma membrane and the Golgi apparatus. At least three unique dynamin gene products have been described that vary in their tissue expression. Dynamin I is expressed predominantly in neurons, while dynamin II is ubiquitously expressed and dynamin III is expressed in the testis, lung, and brain. In addition, each form of dynamin has a variety of alternatively spliced forms, although the specific functions and expression patterns of these isoforms have not all been determined (14, 77).

Here we use a variety of approaches to further define the uptake and infection pathway of CPV into cells. CPV capsids concentrated within electron-dense coated pits on the cell surface and then entered mink lung cells by clathrin-mediated endocytosis. CPV did not significantly permeabilize cells to allow the coentry of the toxin α-sarcin. CPV particles became colocalized with transferrin (Tfn) in endosomes but not with dextran, suggesting that viral particles are delivered to a recycling endosomal compartment after endocytic uptake.

MATERIALS AND METHODS

Viruses and cells. CPV type 2 (CPV-d) was grown in NLFK cells, and aliquots were frozen and stored at −70°C (59). Virus titers were determined on NLFK cells by 50% tissue culture infective dose assay in 96-well plates as described previously (58). Full CPV particles were purified and quantified as previously described (47) and stored in phosphate-buffered saline (PBS) at 4°C. Canine adenovirus type 1 (CAV-1) grown in MDCK cells was purified by banding on CsCl gradients as described by Cotten et al. (20) and then dialyzed against PBS (pH 7.4). CAV-1 particle concentration was determined spectrophotometrically, using a conversion factor of 1.1×10^{12} viral particles per 1 unit of optical density at 260 nm (48). Canine A72 cells and NLFK cells were grown and maintained in a 1:1 mixture of McCoy's 5A and Leibovitz L15 medium with 5% fetal bovine serum (FBS), and tTA-Mv1Lu, Mv1Lu-TR, Mv1-WT, and Mv1-K44A cells were grown in Dulbecco modified Eagle medium (DMEM) containing 10% FBS.

Tetracycline-regulated expression of wild-type and mutant dynamin. tTA-Mv1Lu cells that stably express the tetracycline-responsive transactivator were obtained from Joan Massague (67). Plasmids pUHD10-3 HA-wt and pUHD10-3 HA-ele1 express wild-type dynamin I and a dominant interfering mutant of dynamin I with lysine 44 changed to alanine (K44A), respectively, from a minimal cytomegalovirus promoter under the control of a tetracycline-responsive enhancer element. The genes are fused to a hemagglutinin (HA) epitope tag at the N terminus and were provided by Sandra Schmid (25, 26). tTA-Mv1Lu cells were transfected with 20 μg of either plasmid pUHD10-3 HA-ele1 or plasmid pUHD10-3 HA-wt together with 1 μg of the puromycin resistance plasmid pBSpac, using a Bio-Rad Gene Pulser II with radiofrequency module at 400 V, 85% modulation, 40-kHz radio frequency, and 5 bursts of 4.0-ms duration with a burst interval of 1 ms. Cells were grown in medium containing puromycin (600 ng/ml) and tetracycline (2 μg/ml), and clones were picked after 7 to 10 days. Clones showing strong inducible expression of wild-type and mutant dynamin were further subcloned and designated Mv1-WT and Mv1-K44A, respectively.

Flow cytometry assay of infection. Mv1-K44A or Mv1-WT cells were cultured for 48 h in DMEM with 10% FBS with or without 2 μg of tetracycline per ml. As the growth rate of cells expressing mutant dynamin was slower than that of cells grown in the presence of tetracycline, the Mv1-K44A cells when grown without tetracycline were seeded at a higher density so that all cells were at the same density 48 h later. Cells were incubated with CPV at a multiplicity of infection of 0.3 for 1 h at 37°C; then fresh medium containing tetracycline (2 μg/ml) was added, and the incubation continued for 15 h at 37°C. Cells were then washed in PBS, trypsinized and resuspended in DMEM–10% FBS, rinsed in PBS, and fixed

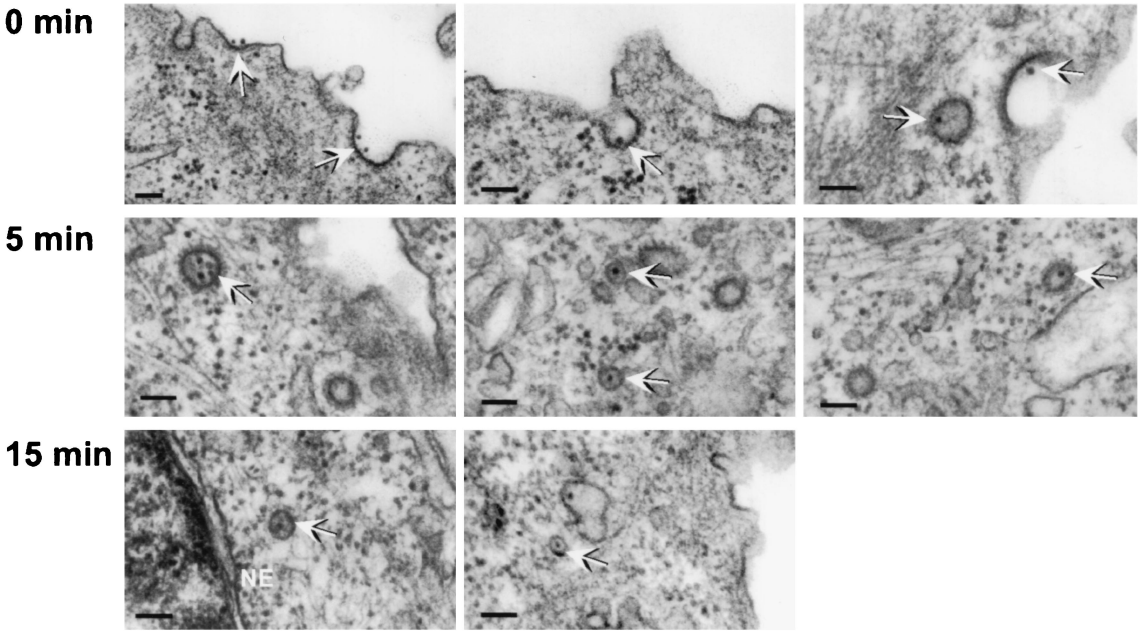

FIG. 1. Electron microscopy of CPV bound to uninduced Mv1-K44A cells at 0, 5, and 15 min after warming from 4 to 37°C. The bars represents 100 nm; arrows indicate likely viral particles. The nuclear envelope (NE) is indicated.

in 2.5% paraformaldehyde in PBS at 20°C for 10 min. Cells were washed in PBS with 0.5% bovine serum albumin (BSA), then permeabilized in PBS-BSA with 0.1% Triton-X100, and incubated with mouse monoclonal antibody (MAb) CE-10 against the C terminus of the MVM nonstructural protein NS1 (obtained from Caroline Astell [85]) for 1 h at room temperature. The antibody was detected with a fluorescein-conjugated goat anti-mouse antibody; then 20,000 cells assayed in a FACScalibur flow cytometer (Becton Dickinson, San Jose, Calif.).

Cell cycle analysis. Mv1-K44A or Mv1-WT cells were cultured for 48 h in DMEM–10% FBS with or without tetracycline (2 μg/ml), isolated in suspension as described above, and then incubated for 20 min at −20°C in 100% methanol. After washing with PBS, the cells were treated with RNase A (1 mg/ml in PBS) for 30 min at 37°C and then incubated with propidium iodide (0.01 mg/ml in PBS) and 0.02% Triton X-100 at 4°C for 30 min. Cell DNA content was assayed by flow cytometry (45). The data from four independent experiments were modeled, and the percentage of cells in each phase of the cell cycle was estimated with ModFit LT cell cycle analysis software (Verity Software, Topsham, Maine).

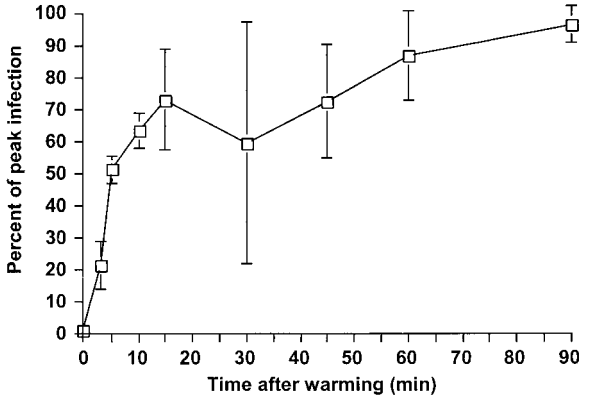

FIG. 2. Kinetics of uptake of infectious CPV from the cell surface. Virus was bound to tTA-Mv1Lu cells at 4°C, and then the cells were rapidly warmed to 37°C. At various times after warming, neutralizing anti-CPV antibody was added and mixed with the medium. The percentages of infected cells in each dish were assayed 24 h later by immunostaining and flow cytometry. The average and standard deviations of the percent maximal infection of four separate experiments are shown.

Electron microscopy. Cells grown for 24 h on Thermanox 13-mm-diameter coverslips (Nunc Inc., Naperville, Ill.) were washed once in ice-cold DMEM and CPV-d full particles (35 μg/ml) were incubated on the cells for 1 h at 0°C (1 μg of CPV-d full particles is equivalent to $\sim 10^{11}$ particles). Immediately after incubation at 0°C or at 5 and 15 min after warming to 37°C, the cells were fixed in 1% glutaraldehyde–0.1 M sodium cacodylate (pH 7.4) for 30 min at room temperature and then for 1.5 h on ice in 2.5% glutaraldehyde in 0.1 M sodium cacodylate (pH 7.5). After being rinsed three times in ice-cold cacodylate buffer, cells were postfixed in 4% osmium tetroxide for 1 h at room temperature, stained for 20 min with a 2% aqueous solution of uranyl acetate, and then dehydrated with ethanol. The cells were embedded in Epon-Araldite plastic; thin sections were cut and further stained for 20 min in 2% aqueous uranyl acetate, rinsed, stained with lead citrate for 7 min, and then examined in a Philips 201 electron microscope. The numbers of particles associated with coated and noncoated regions of the plasma membrane at the 0-min time point were counted.

Virus binding to cells. Mv1-WT and Mv1-K44A cells cultured with or without tetracycline for 48 h were washed with PBS and then treated with a nonenzymatic cell dissociation solution (Sigma, St. Louis, Mo.) for 15 min at 37°C. Cells were washed in DMEM–10% FBS and then incubated in cold DMEM–1% BSA on ice for 10 min. The cells were pelleted at 4°C and then resuspended in DMEM–1% BSA or in DMEM–1% BSA containing 40 μg of full CPV per ml. After incubation on ice for 1 h, the cells were washed three times with ice-cold PBS, fixed in 2% paraformaldehyde and PBS for 10 min on ice, and then immunostained with a MAb 8 against the intact capsid protein (71). The cells were then washed with PBS, permeabilized with 0.1% Triton X-100 in PBS, and immunostained for the HA epitope tag with a rabbit polyclonal antiserum (Santa Cruz Biotechnology, Inc., Santa Cruz, Calif.). Primary antibodies were detected with fluorescein isothiocyanate (FITC)-conjugated goat anti-rabbit and R-phycoerythrin-conjugated goat anti-mouse secondary antibodies (Jackson Immunoresearch, West Grove, Pa.). Viral binding and HA epitope tag expression were assessed by flow cytometry.

Kinetics of CPV infectious entry. tTA-Mv1Lu cells grown on 60-mm-diameter dishes were incubated with CPV at an multiplicity of infection of 0.3 for 2 h on ice, washed once in cold DMEM to remove unbound virions, and then warmed to 37°C by the addition of prewarmed DMEM–10% FBS. After various times of incubation, a rabbit anti-CPV neutralizing antiserum was added and mixed with the medium. Mock-inoculated cells were also treated with antibody. The cells were then incubated for 24 h at 37°C, fixed, and assayed for infection by staining for NS1 expression as described above.

Control markers of endocytosis. Human Tfn (HuTfn) did not bind Mv1-K44A cells, so we used a cDNA for the HuTfn receptor (HuTfnR) to express the human receptor in those cells. Cells transfected by electroporation were seeded onto glass coverslips in the presence or absence of tetracycline. After 48 h, cells were washed and incubated in DMEM–1% BSA for 45 min at 37°C and then incubated for 10 minutes at 37°C with Texas red-labeled HuTfn (50 μg/ml; Molecular Probes, Eugene, Oreg.) in DMEM–1% BSA. After washing with PBS,

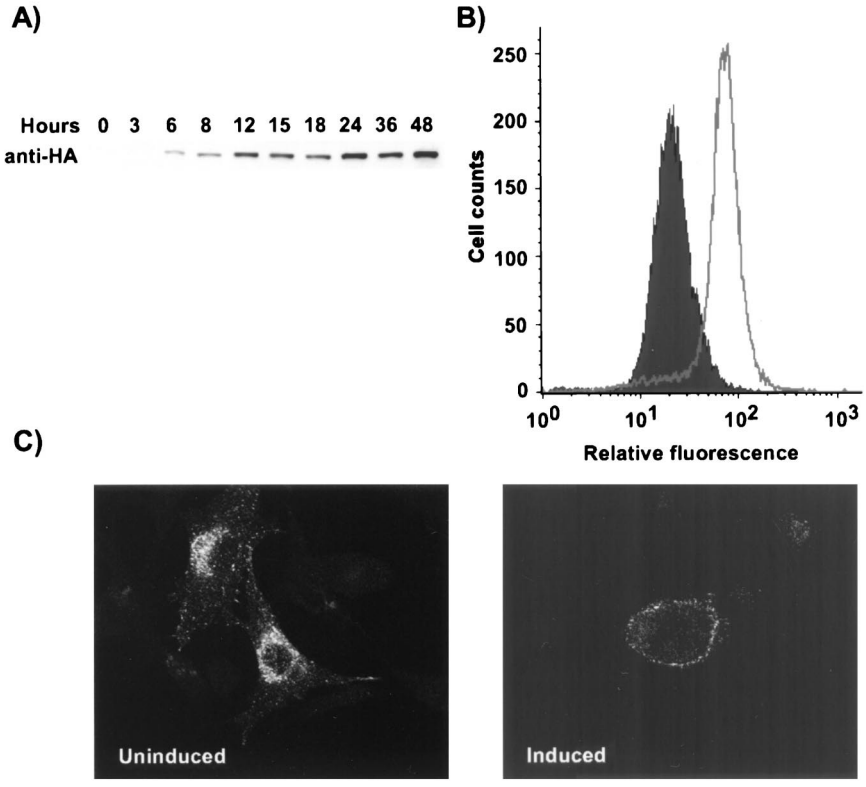

FIG. 3. Characterization of Mv1-K44A cells. (A) Western blot analysis of dynamin K44A expression in Mv1-K44A cells at various times after tetracycline removal. The dynamin K44A was detected with MAb 12CA5 against the N-terminally fused HA epitope. (B) Expression of dynamin K44A in Mv1-K44A cells. Cells grown with or without tetracycline for 48 h were harvested for flow cytometry. The HA-tagged dynamin was detected by indirect immunofluorescent staining with MAb 12CA5, and 20,000 cells were analyzed by flow cytometry. (C) Uptake of HuTfn by induced and uninduced Mv1-K44A cells. Mv1-K44A cells transfected with the HuTfnR gene were grown in the presence or absence of tetracycline for 48 h on coverslips. Texas red-labeled HuTfn was incubated with the cells for 10 min at 37°C prior to fixation and examination by fluorescence microscopy.

the cells were fixed for 10 min in 2.5% paraformaldehyde in PBS, rinsed three times in PBS, then mounted on slides with Prolong (Molecular Probes), and examined by confocal microscopy (25).

Fluid-phase endocytosis was examined by following the uptake of FITC-dextran (10,000 Da, lysine fixable; Molecular Probes). Cells were washed twice in DMEM–1% BSA and then incubated with FITC-dextran (2 mg/ml) at 37°C for 20 min. The cells were then chilled on ice, washed four times with ice-cold PBS, fixed with 3% paraformaldehyde for 15 min, washed, and examined by fluorescence microscopy (25).

Immunofluorescence microscopy. Mv1-K44A cells were seeded onto glass coverslips at a cell density of 1.2×10^4 or $2 \times 10^4/cm^2$ with or without tetracycline (2 μg/ml), respectively. After 48 h, the cells were cooled on ice and incubated with purified CPV full particles (20 μg/ml in DMEM) for 1 h, and then unbound virus was removed by washing with ice-cold DMEM. After warming to 37°C, the cells were incubated for 10, 30, or 90 min, washed three times in ice-cold PBS, and then fixed with 2.5% paraformaldehyde in PBS. Cells were permeabilized with 0.1% Triton X-100 in PBS-BSA, and the capsids were detected either with MAb 8 followed by a Cy3-labeled donkey anti-mouse secondary conjugate (Jackson Immunoresearch) or with a rabbit polyclonal anticapsid serum followed by goat anti-rabbit antibody-FITC conjugate. Confocal optical sections through the center of the cells were collected using a Bio-Rad MR600 confocal system. Single optical sections of approximately 2.2-μm thickness are shown.

Detection of CPV together with HuTfn and dextran in tTA-Mv1Lu cells. tTA-Mv1-Lu cells were transfected with 20 μg of plasmid pCB6 HuTfnR together with 1 μg of pBSPac by electroporation as described above and then seeded into 100-mm-diameter dishes. Stable clones were selected with puromycin (600 ng/ml) as described above. A clone of cells which bound and endocytosed HuTfn was chosen for further use and designated Mv1Lu-TR.

Mv1Lu-TR cells seeded on coverslips were washed with DMEM–1% BSA and then incubated with DMEM–1% BSA for 45 min at 37°C to remove endogenous Tfn from the receptors. The coverslips were then inoculated with purified CPV full particles (20 μg/ml) and Texas red-labeled HuTfn (100 μg/ml) in DMEM–1% BSA and incubated at 37°C for 2 h. After washing with ice-cold PBS, cells were fixed and permeabilized as described above, and then capsid proteins were detected by staining with MAb 8 followed by goat anti-mouse antibody-FITC.

To examine co-uptake of CPV and dextran, purified capsids were bound to uninduced or induced Mv1-K44A cells on coverslips as described above. After washing in ice-cold DMEM–1% BSA, the coverslips were incubated with 2 mg of lysine-fixable FITC-conjugated dextran (molecular weight, 10,000) per ml in DMEM–1% BSA for 15 min at 37°C. The coverslips were washed extensively in ice-cold PBS and fixed for 2 h in 4% paraformaldehyde in PBS. To detect capsid proteins, the cells were briefly permeabilized with 0.05% saponin in PBS–2% BSA and immunostained with MAb 8 followed by donkey anti-mouse antibody-Cy3 conjugate, and confocal sections were collected through the center of the cells.

Effect of BFLA1. In initial studies, we determined that 10 nM bafilomycin A1 (BFLA1) inhibited viral infection by 98% when added 30 min prior to virus inoculation. To further examine the effect of BFLA1 on infection, the drug was therefore added to cells either 30 min before or 90 min after virus incubation. tTA-Mv1Lu cells seeded at $2 \times 10^4/cm^2$ in 60-mm-diameter dishes were cultured overnight, preincubated with DMEM alone or DMEM containing 20 nM BFLA1 for 30 min at 37°C, and then incubated with CPV with or without 20 nM BFLA1 for 1 h at 37°C. The cells were washed in DMEM and then in DMEM–10% FBS or DMEM–10% FBS with 20 nM BFLA1 added. In some cases, 20 nM BFLA1 was added to the medium 30 min after removal of virus inoculum. Controls were mock-inoculated cells or cells inoculated without BFLA1. Cells were harvested by trypsinization, and then virus infection was assayed by staining the cells for NS1 expression as described above.

In other experiments tTA-Mv1Lu cells seeded on coverslips were incubated with 20 or 200 nM BFLA1 in DMEM–1% BSA for 30 min at 37°C, incubated for 20 min with 10 mg of FITC-dextran per ml in DMEM, and then fixed in 2.5% paraformaldehyde in PBS for 30 min. Other cells treated with 20 or 200 nM BFLA1 for 30 min at 37°C were chilled and incubated with 20 μg of purified full CPV particles (with BFLA1) per ml for 1 h on ice, rewarmed to 37°C for 10 min, and fixed in 2.5% paraformaldehyde in PBS for 10 min; then capsids were stained with MAb 8 followed by a goat anti-mouse antibody-FITC conjugate. Control cells were incubated with virus and FITC-dextran without BFLA1. Images were collected by confocal microscopy as described above.

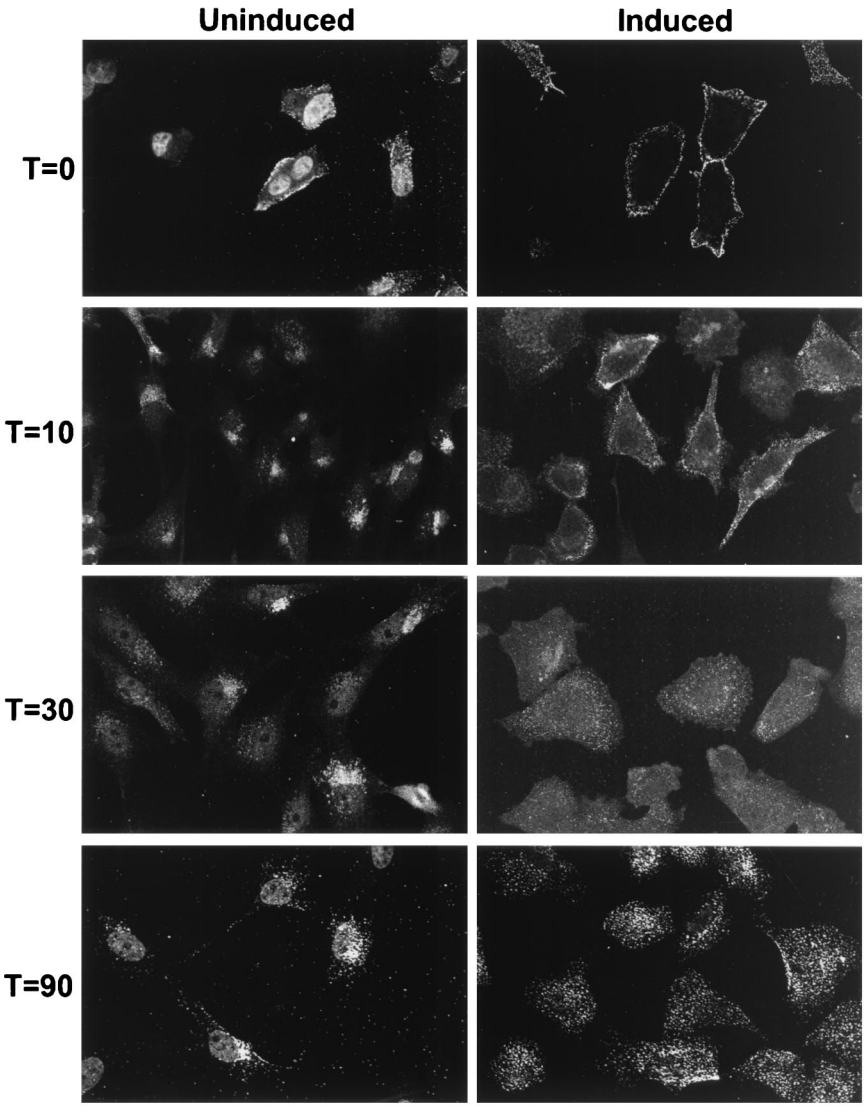

FIG. 4. CPV uptake into vesicles in uninduced and induced Mv1-K44A cells. Purified CPV full particles were incubated with uninduced or induced Mv1-K44A cells for 1 h at 4°C. The cells were then fixed immediately or after 10, 30, or 90 min of incubation at 37°C. CPV particles were detected by indirect immunofluorescence using a rabbit anticapsid antibody, and confocal images were collected. Because of lower binding of CPV to uninduced cells, images of uninduced cells at time zero were collected using a higher gain than those of the induced cells, and as a result nonspecific nuclear fluorescence is also seen.

Cell permeabilization assay. The ability of CPV to permeabilize A72 or tTA-Mv1Lu cells to the translation-inhibiting toxin α-sarcin was assessed as described by Cuadras et al. (22). In brief, purified full CPV at between 2×10^{10} and 1×10^{13} particles per ml or purified CAV-1 at between 4.4×10^{8} and 4.4×10^{10} particles per ml was added to confluent A72 cells or tTA-Mv1Lu cells seeded in 1-cm^2 wells. After incubation at 37°C for 90 min with or without α-sarcin (100 μg/ml), the cells were washed in PBS, incubated with [^{35}S]methionine for 1 h at 37°C, then washed with PBS, and incubated with 5% trichloroacetic acid for 5 min at room temperature. After washing the cells three times with ethanol they were dried and recovered into 0.1 ml of 0.1% sodium dodecyl sulfate in 0.1 M NaOH, and the incorporated [^{35}S]methionine was measured by liquid scintillation counting.

RESULTS

Electron microscopy indicates virus binding to coated pits. Virus cell binding and uptake were examined by transmission electron microscopy. At 0 min, 67% (281 of 419 particles counted) of viral particles seen bound to the plasma membrane were in depressions that had an electron-dense coating resembling clathrin-coated pits; 5 min after warming, most viral particles were found in coated vesicles but some were in noncoated vesicles; by 15 min, most viral particles were seen within noncoated vesicles, some of which appeared to be close to the nuclear membrane (Fig. 1).

CPV particles bound on the cell surface rapidly become resistant to neutralizing antibody upon warming. Assays based on postadsorption neutralization of virus have demonstrated that the infectious entry of SV40 virus is slow and occurs in hours, while adenovirus entry occurs in minutes (2, 79). We used a similar assay to determine the kinetics of CPV removal from the surface of mink lung cells. The virus rapidly became resistant to antibody, and 50% of the infecting virus entered the cell by 5 min after warming (Fig. 2). These results are consistent with our finding that virus bound to coated pits.

Characterization of tTA-Mv1Lu cells which inducibly express wild-type dynamin or mutant dynamin K44A. Overexpression of dynamin K44A in cells inhibits clathrin-mediated endocytosis (26). We prepared and cloned two tTA-Mv1Lu

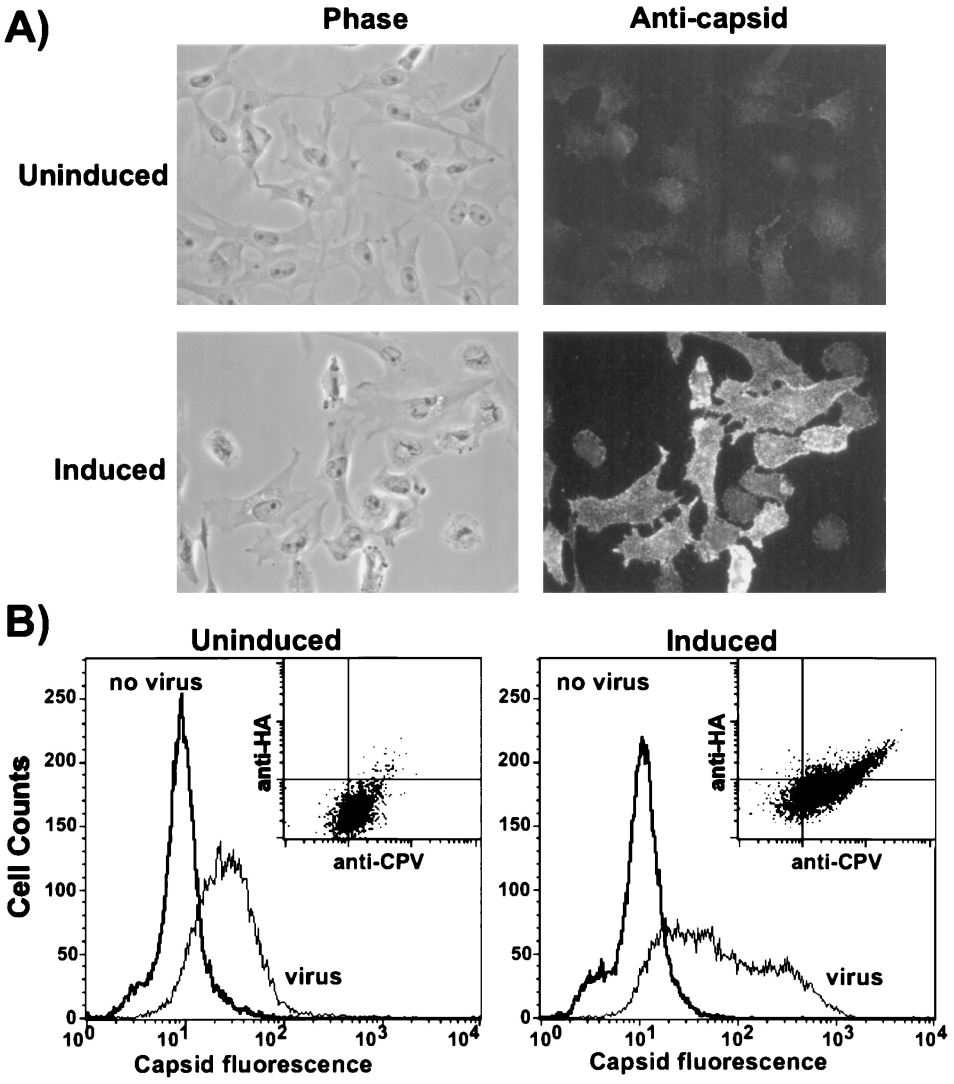

FIG. 5. Binding of full CPV particles to uninduced and induced Mv1-K44A cells. (A) Purified CPV full particles were bound to uninduced or induced Mv1-K44A cells for 1 h at 4°C; then the cells were fixed, and capsids were detected by indirect immunofluorescence with MAb 8. Phase-contrast images are shown in the left panels. The two fluorescence images were collected using identical exposures. (B) Mv1-K44A cells grown in the presence or absence of tetracycline were suspended by treatment with EDTA and then incubated for 1 h on ice with or without 40 μg of full CPV particles per ml. After washing, the cells were fixed and immunostained for capsid and then permeabilized, and the dynamin K44A was immunostained using the fused HA epitope tag. Cell-associated fluorescence was determined by flow cytometry for each sample. The histograms shows the binding of CPV to the cell surface. The inset is a dot plot showing the binding of CPV versus expression of the HA tag.

cell lines which inducibly expressed either wild-type dynamin (Mv1-WT) or dynamin K44A (Mv1-K44A) in response to removal of tetracycline from the growth medium, similar to that described for HeLa cells (26). In Mv1-K44A cells grown without tetracycline, dynamin expression was first detected 6 h later, and the amount detected increased over 48 h (Fig. 3A). Results for Mv1-WT cells were similar (data not shown). Experiments with dynamin-expressing cells were therefore carried out after a 48-h induction period.

The induced Mv1-K44A cells uniformly expressed dynamin K44A after 48 h (Fig. 3B), and by light microscopy the induced cells were more rounded and had fewer cytoplasmic extensions than uninduced cells, as was seen for HeLa cells expressing dynamin K44A (25).

Tfn uptake was used as a marker of clathrin-mediated endocytosis (25). As HuTfn did not bind Mv1-K44A cells, we transfected the cells with a plasmid expressing the HuTfnR and then examined the uptake of Texas red-labeled HuTfn. After 10 min at 37°C, HuTfn was found predominantly in perinuclear vesicles in uninduced cells, whereas in the dynamin K44A-expressing cells it was located close to the plasma membrane (Fig. 3C). These results indicate that dynamin K44A inhibited clathrin-mediated endocytosis in the induced Mv1-K44A cells as reported for HeLa cells (25). Uptake of the fluid-phase marker FITC-dextran was morphologically similar in both uninduced and induced Mv1-K44A cells (data not shown).

Vesicular uptake of CPV particles was delayed in dynamin K44A-expressing cells. The location of viral particles in induced or uninduced Mv1-K44A cells was examined by immunofluorescence. Cells fixed immediately after incubation with virus on ice showed cell surface localization of viral particles in both induced and uninduced cells; after 10 min at 37°C viral particles were found in large, perinuclear vesicles in uninduced cells, while in dynamin K44A-expressing cells the vesicles re-

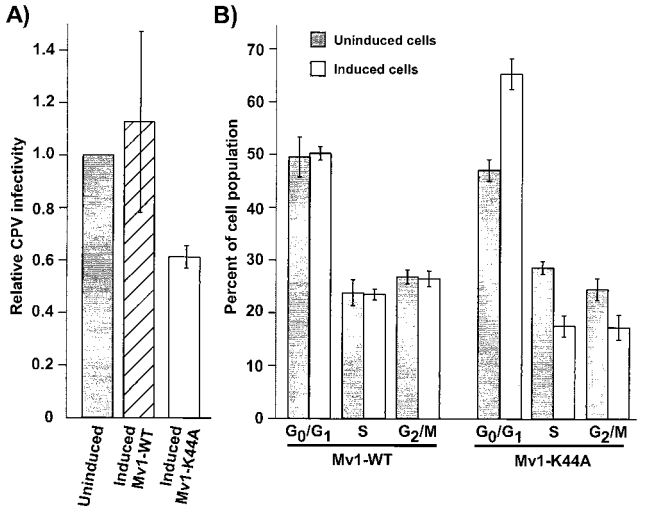

FIG. 6. CPV infection and cell cycle analysis of uninduced and induced Mv1-WT and Mv1-K44A cells. (A) Mv1-WT and Mv1-K44A cells grown with or without tetracycline for 48 h were inoculated with CPV, and the percentage of infected cells was assayed after 16 h by anti-NS1 staining and flow cytometry. The results are expressed as the percentage of cells infected in the induced culture relative to the percentage of cells infected in uninduced cultures. The average and standard deviation of three independent experiments are shown. Each experiment had a minimum of three replicates. (B) Mv1-WT and Mv1-K44A cells grown with or without tetracycline for 48 h were analyzed for DNA content by propidium iodide staining and flow cytometry. The percentage of cells in each phase of the cell cycle was estimated with Modfit LT cell cycle analysis software. Results shown are the average and standard deviation of four independent experiments.

mained close to the cell surface; after 30 and 90 min at 37°C, the viral particles remained in perinuclear vesicles in the uninduced cells, while the virus-containing vesicles in the dynamin K44A-expressing cells had moved centripetally toward the nucleus (Fig. 4). These results show that expression of dynamin K44A disrupted the normal rapid trafficking of CPV to a perinuclear location within cells. However, the gradual centripetal movement of viral particles may indicate that dynamin K44A expression induced a kinetic block rather than an absolute block to vesicle formation and trafficking.

Dynamin K44A expression enhances CPV binding but causes cell cycle arrest and reduces infection. By fluorescence microscopy, more CPV particles appeared to bind to induced Mv1-K44A cells than to uninduced cells (Fig. 5A). By flow cytometry, we found that up to 10-fold more viral particles bound to many of the dynamin K44A-expressing Mv1-K44A cells than to uninduced cells (Fig. 5B). The induced Mv1-K44A cells which bound more virus represented approximately 40% of the total population of cells, and this population of cells also expressed more dynamin as indicated by increased HA epitope expression (Fig. 5B, inset). We found no difference in CPV binding to induced or uninduced Mv1-WT cells (data not shown).

As there was a clear difference in CPV particle uptake between uninduced and induced Mv1-K44A cells, we compared the efficiency of CPV infection of those cells to the efficiency of infection in uninduced and induced Mv1-WT cells. We found that between 8 and 25% of the uninduced Mv1-K44A cells became infected, while the dynamin K44A-expressing cultures had 40% fewer infected cells on average than the uninduced cultures (Fig. 6A). In contrast, there was no significant difference in the infection rate of induced and uninduced Mv1-WT cells. As CPV replicates only in cells that enter the S phase of the cell cycle, we examined the cell cycle distribution of uninduced and induced Mv1-WT and Mv1-K44A cells at the time of virus inoculation. On average, there were 39% fewer cells in S phase, 39% more cells in G_0/G_1, and 30% fewer cells in G_2-M in the induced Mv1-K44A cells than in the uninduced cells at the time of virus inoculation, whereas in the Mv1-WT cells there was no difference in the cell cycle distribution of induced and uninduced cells (Fig. 6B).

CPV colocalizes with Tfn in a perinuclear vesicular compartment but not with dextran. To examine virus trafficking, we stably transfected tTA-Mv1Lu cells with the HuTfnR (Mv1Lu-TR cells) and examined the localization of virus and Tfn in these cells. After 2 h at 37°C, HuTfn and CPV particles clearly colocalized to perinuclear vesicles in the Mv1Lu-TR cells (Fig. 7A). In contrast, virus and FITC-dextran showed little colocalization in the uninduced Mv1-K44A cells (Fig. 7B). In the induced Mv1-K44A cells the dextran was observed in endosomal vesicles, while the virus remained associated with the plasma membrane (Fig. 7C).

BFLA1 inhibited CPV infection. Previous studies of CPV entry have shown that treatment of cells with ammonium chloride or chloroquine prevents viral infection (8). BFLA1 at micromolar concentrations specifically inhibits the vacuolar proton ATPase, preventing acidification of endosomes (11), and it also inhibits transport from early to late endosomes in HeLa cells (10). However, Bayer et al. found only a small increase (0.2 pH units) in the intravesicular pH of HeLa cells treated with 20 nM BFLA1 (10). We found that addition of 10 nM BFLA1 to NLFK and A72 cells 30 min before inoculation with virus reduced the 50% tissue culture infective dose titer measured 48 h later by 95% in NLFK cells and 98% in A72 cells (data not shown). There was a 96% reduction in the infection rate of tTA-Mv1Lu cells treated with 20 nM BFLA1 30 min prior to incubation with virus and a 71% reduction when BFLA1 was added 90 min after virus inoculation (Fig. 8A). The cell cycle distribution of tTA-Mv1Lu cells treated with 100 nM BFLA1 for 16 h was no different from that of untreated cells (data not shown). From these data, we conclude that 20 nM BFLA1 inhibits CPV infection of tTA-Mv1Lu cells and that this inhibition was not due to an indirect effect of BFLA1 on the cell cycle.

As it was unlikely that 20 nM BFLA1 treatment caused a significant increase in endosomal pH, we investigated the possibility that BFLA1 treatment of tTA-Mv1Lu cells influenced the endocytic trafficking of viral particles. Bayer et al. reported that 200 nM but not 20 nM BFLA1 affected the endocytic transport of dextran and human rhinovirus 2 in HeLa cells (10). In contrast, we found that treatment of tTA-Mv1Lu cells with 20 nM BFLA1 changed the vesicular distribution of viral particles after 10 min of uptake at 37°C (Fig. 8B). The majority of virus-containing vesicles in untreated cells were located close to the Golgi in the perinuclear cytoplasm, whereas in cells treated with 20 or 200 nM BFLA1 the virus-containing vesicles were dispersed throughout the cytoplasm (Fig. 8B). The 20 nM BFLA1 treatment had little effect on the distribution of FITC-dextran-containing vesicles, which were found in the perinuclear cytoplasm after 20 min at 37°C (Fig. 8B). However, treatment with 200 nM BFLA1 did alter the distribution of FITC-dextran, which was seen in smaller vesicles that were distributed more widely throughout both the perinuclear and peripheral cytoplasm (Fig. 8B).

CAV-1 but not CPV particles permeabilized cells to α-sarcin. Human adenovirus type 2, poliovirus, and rotavirus are nonenveloped viruses that are known to permeabilize host cells and permit the entry of certain proteins or toxins (29, 30). Coincubation of A72 cells with 10^{13} particles of CPV per ml

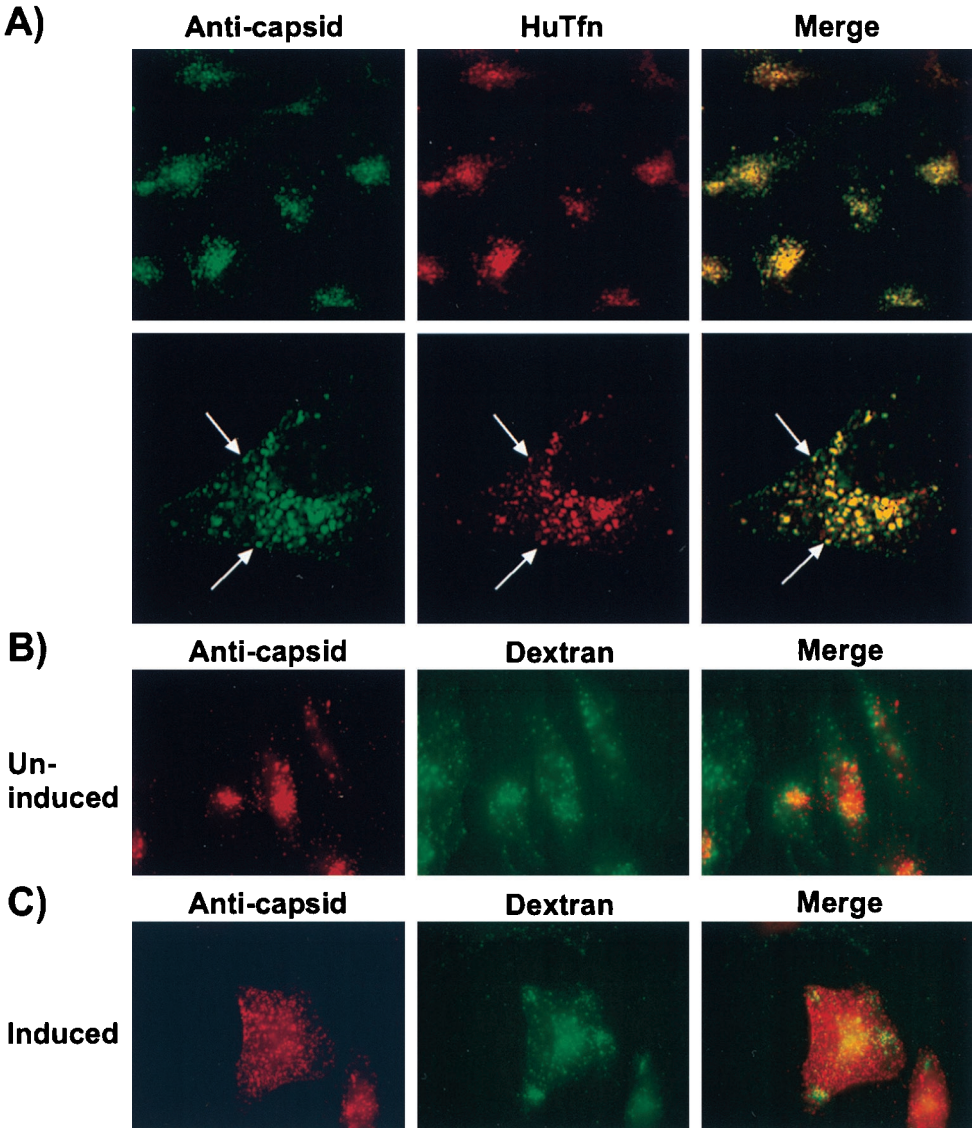

FIG. 7. Confocal images showing co-uptake of CPV and Texas red HuTfn in Mv1Lu-TR cells or of CPV and FITC-dextran in uninduced and induced Mv1-K44A cells. (A) Mv1Lu-TR cells stably expressing the HuTfnR were incubated with full CPV particles and Texas red-labeled HuTfn for 2 h at 37°C. Capsids were detected with MAb 8. The upper panels show a 630× magnification; the lower panels show a 1500× magnification of a single cell. The arrows indicate individual vesicles containing virus and Tfn. Mv1-K44A cells grown for 48 h with (B) or without (C) 2 μg of tetracycline per ml were incubated with full CPV particles for 1 h at 4°C and then warmed to 37°C by the addition of warm DMEM–1% BSA containing 2 mg of lysine-fixable FITC-dextran per ml. After incubation at 37°C for 15 min, the cells were fixed and permeabilized, and capsids were detected with MAb 8.

and 100 μg of α-sarcin per ml resulted in an insignificant decrease in [^{35}S]methionine incorporation, while adding 2.5×10^{10} particles of CAV-1 per ml with 100 μg of α-sarcin per ml resulted in a 89% decrease in incorporation of [^{35}S]methionine (Fig. 9). Results were similar when the experiment was carried out in tTA-Mv1Lu cells (Fig. 9). In both cell lines, the degree of permeabilization to α-sarcin by CAV-1 particles increased with increasing amounts of virus, but no change was seen with increasing amounts of CPV.

DISCUSSION

Here we have defined several steps in the capsid uptake and infection pathway of CPV which have not been previously reported. This small and very stable virus enters cells and transports its DNA to the nucleus for replication. The success of cell infection can vary more than 10^6-fold, depending on the host of origin of the cell and on the presence of single or double amino acid substitutions in the surface of the virus capsid (15, 58, 76). The host range mutations affect infection after virus binding to the cell surface but before DNA replication (38, 58).

Virus and its receptor enters cells via dynamin-mediated endocytosis. We have demonstrated that uptake of viral particles from the plasma membrane occurred rapidly via clathrin-coated vesicles. This was shown by the rapid removal of virus from the cell surface, by the localization and concentration of the particles within coated pits and vesicles, and also by the observation that uptake and transport of virus-containing vesicles were strongly inhibited by overexpression of dynamin K44A mutant in the cells.

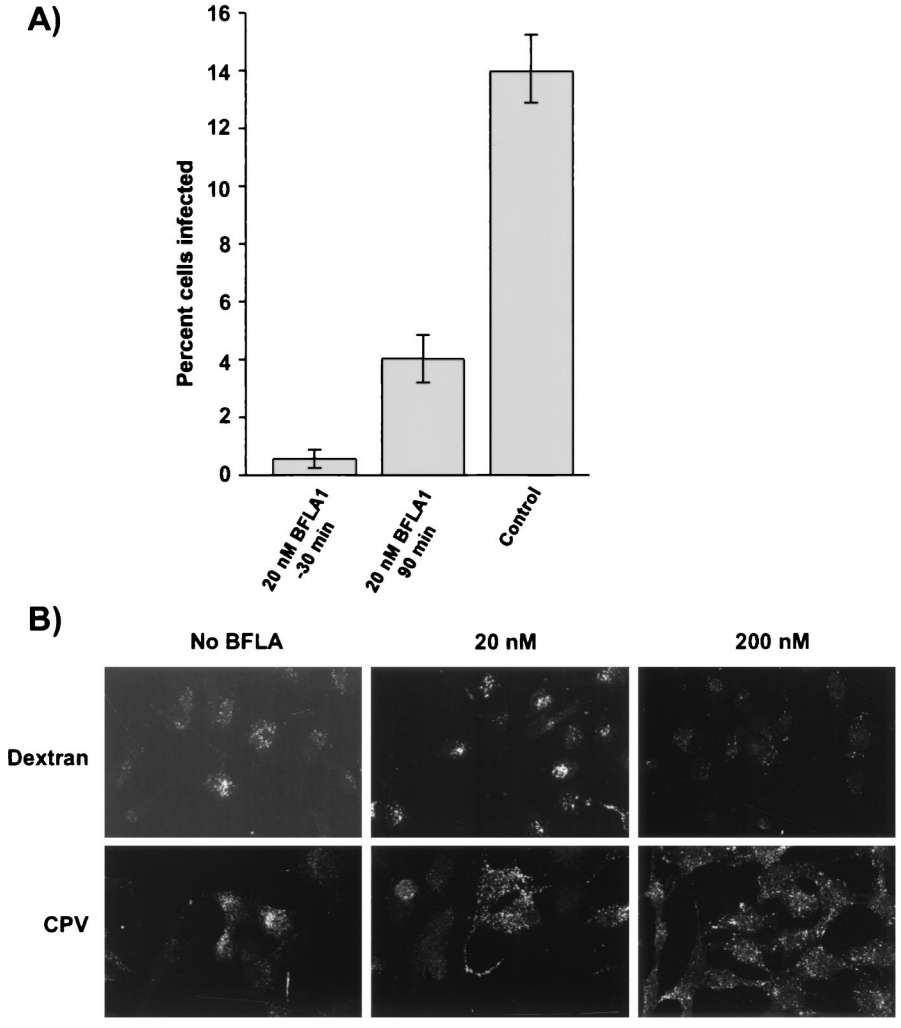

FIG. 8. Effect of BFLA1 on CPV infection and the distribution of virus-containing vesicles in tTA-Mv1Lu cells. (A) BFLA1 (20 nM) was added to tTA-Mv1Lu cells either 30 before virus incubation or 90 min after inoculation and then maintained with the cells for a further 16 h. Control cells were inoculated but not treated with BFLA1. Cells were trypsinized, fixed, and immunostained for flow cytometry. Results shown are the average and standard deviations from three replicates. (B) tTA-Mv1Lu cells grown on coverslips were treated for 30 min with 20 or 200 nM BFLA1 at 37°C, and then full CPV particles (20 μg/ml) were bound to the cells for 1 h on ice in the presence of the drug. After washing in cold PBS, the cells were warmed to 37°C for 10 min. Similarly, 10 mg of FITC-dextran per ml was added for 20 min to cells treated with 20 or 200 nM BFLA1 for 30 min at 37°C. After washing in cold PBS, the cells were fixed and capsids detected with MAb 8. Confocal images are shown.

In a previous study, it was reported that most CPV particles were seen within noncoated endosomes in A72 cells 15 min after uptake, and it was suggested that CPV entered those cells by a non-clathrin-mediated pathway (8). We found that in cells fixed at 0 and 5 min after warming, the majority of capsids (67% at time zero) seen were within coated pits or vesicles at or close to the cell surface, while at 15 min virus was also seen in noncoated vesicles in the peripheral and perinuclear cytoplasm. It is likely that in the previous study the clathrin coat had been lost from virus-containing vesicles, as clathrin coats may be removed from vesicles within 1 to 3 min after pinching off from the plasma membrane (55).

The rapid uptake of the particles into a compartment inaccessible to neutralizing antibody also indicates that infectious entry involves clathrin-mediated pathways. Rapid uptake of ligands is characteristic of clathrin-mediated endocytosis (55). In contrast, SV40 was found to enter and infect cells through caveolae and to require 2.5 h for 50% of the bound virus to be removed from the cell surface (2). Dynamin may also be involved in budding of caveolae from the plasma membrane (37). However, the rapid uptake of infecting CPV indicates that caveolae were not involved, as uptake of ligands by caveolae is characteristically slow (3). In addition, we have found that treatment of cells with nystatin, an inhibitor of caveola formation (2), does not affect CPV infection (J. Parker and C. Parrish, unpublished data). Therefore, the effect of dynamin K44A expression on CPV uptake and infection is most likely due to inhibition of clathrin-mediated endocytosis.

The effects of the dynamin K44A expression on virus uptake and infection of cells are complex, as many normal cellular functions depend on efficient endocytosis regulated by dynamin (1, 32, 40, 80, 86). Although the dynamin K44A clearly prevented efficient transport of virus-containing vesicles from the plasma membrane, the virus-containing vesicles moved slowly into the cytoplasm. It has been reported that in HeLa cells expressing dynamin K44A, long clathrin-coated tubes can extend from the plasma membrane deep into the cell (25). In addition, although Tfn uptake in dynamin K44A-expressing

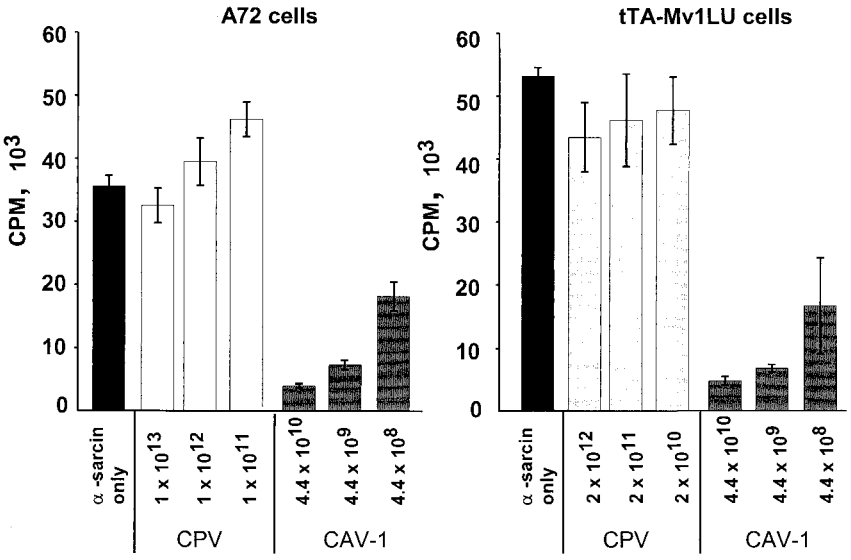

FIG. 9. Effect of CAV-1 or CPV capsids on the permeability of cells to the protein synthesis inhibitor α-sarcin. CPV full capsids or CAV-1 particles at the concentrations shown (particles per milliliter) were incubated with A72 or tTA-Mv1Lu cells with or without 100 μg of α-sarcin per ml for 90 min at 37°C and then incubated with [^{35}S]methionine for an additional 1 h. Incorporated [^{35}S]methionine was measured by scintillation counting. Results are expressed as the mean and standard deviation of three separate dishes.

HeLa cells was reduced by >80% after 15 min, there was a time-dependent increase in the percentage of bound Tfn that entered these cells (25). Thus, CPV entry may not be completely blocked in induced Mv1-K44A cells, but the kinetics of virus uptake and infection may be slowed. Overexpression of mutant dynamin increases fluid-phase endocytosis (24), but as we did not observe significant colocalization of viral particles and the fluid-phase marker dextran in either induced or uninduced cells (Fig. 7), it appears that CPV capsids do not enter cells by that process.

The increased binding of CPV to the surface of induced Mv1-K44A cells is likely due to an increase in the amounts of cell surface receptors, which is related to the level of dynamin K44A expression. As the plasma membrane concentration of many receptors depends on a balance between receptor addition to the plasma membrane by recycling and synthesis and removal by endocytosis, inhibition of clathrin-mediated endocytosis during the 48 h of induction may have prevented the normal recycling of the CPV receptor, resulting in increased amounts on the plasma membranes. The plasma membrane concentration of the GLUT4 insulin receptor increased with coexpression of dynamin K44A in primary rat adipose cells, and all of the GLUT4 receptors were on the plasma membrane after 24 h of dynamin K44A expression (1).

Over 90% of the cells expressed the dynamin K44A after induction by growth without tetracycline, and there was a 40% reduction in virus infection in the induced Mv1-K44A cells (Fig. 6A), similar to what has been reported for adenovirus infection of HeLa cells (82). However, this result must be interpreted together with our finding that there was a 35 to 40% reduction in the number of cells in the S phase of the cell cycle in the induced cells, which would reduce the number of cells permissive for viral replication (Fig. 6B), while the increased virus binding would likely increase the efficiency of virus infection through any endosomes that were formed (Fig. 5).

Later stages of virus entry and endosomal trafficking are blocked by BFLA1 treatment of cells. Twenty nanomolar BFLA1 inhibited CPV infection by >95% when added to cells prior to virus addition but also resulted in a 70% reduction in infection when added to cells 90 min after the virus (Fig. 8A). In addition, we observed a clear alteration of the distribution of virus-containing vesicles in cells treated with 20 or 200 nM BFLA1 compared to untreated cells (Fig. 8B). This suggests that although viral particles rapidly enter cells within vesicles, the majority of particles remain within endosomal compartments for up to 90 min after uptake. When we examined the effect of 20 or 200 nM BFLA1 on the distribution of FITC-dextran-containing vesicles in tTA-Mv1Lu cells, we saw no difference between treated cells and the untreated control at 20 nM, but there were obvious differences in vesicle distribution in cells treated with 200 nM BFLA1, as has been reported for HeLa cells (10). The difference between the vesicular trafficking of viral particles and FITC-dextran in cells treated with 20 nM BFLA1 is likely to be due to differential effects of BFLA1 on fluid-phase versus receptor-mediated endocytosis. Cell infection by many viruses is inhibited by BFLA1 (10, 35, 52). In micromolar amounts, BFLA1 inhibits the vacuolar proton pump and prevents acidification of endosomes, and it blocks cell infection by adenoviruses, reoviruses, and certain picornaviruses (52, 62, 63). However, treatment of HeLa cells with 20 nM BFLA1 has minimal effects on endosomal pH (10). We do not know what effect 20 nM BFLA1 had on the endosomal pH of tTA-Mv1Lu cells. BFLA1 treatment inhibits early to late endosomal vesicular transport in some cells (10, 17) and affects the recycling of Tfn (39, 64). It is therefore unclear whether the inhibition of CPV infection that we observed was due to an effect of BFLA1 on vesicle pH or on trafficking, or both. Interestingly, the microtubule-destabilizing drug nocodazole inhibits CPV infection when added at 60 min but not at 120 min after virus uptake (81). These results suggest that capsids entering the cell are sequestered in a vesicular compartment and may be only gradually trafficked to another compartment from which they enter the cytoplasm and infect the cell.

Entry of CPV does not result in permeabilization of cells to α-sarcin. At some stage in infection, the CPV capsid must penetrate a membrane barrier to deliver its genome into the cytoplasm of the host cell, prior to delivery to the nucleus. It is not known whether the intact CPV particle passes through the endosomal membrane or whether perhaps pores are formed through which the DNA can pass. The toxin α-sarcin has been used to examine the effects of virus capsids on cell membrane permeability (22, 29, 52). Even very large amounts of CPV capsids did not significantly increase the permeability of the endosomes of mink or canine cells to α-sarcin (Fig. 9), while CAV-1 gave over 90% inhibition of translation, similar to the results reported for the human adenoviruses (30, 62). Adenovirus particles lyse an early endosomal compartment in response to receptor binding and low pH, allowing the entry of other molecules, including α-sarcin, or DNA into the cell cytosol (21, 29).

These results may indicate that the cytoplasmic entry of CPV occurs slowly or at very low levels; that the capsid forms only a small pore through the endosomal membrane for delivery of its DNA, which does not allow the α-sarcin to pass through; that CPV penetrates from the late endosome or lysosome where the toxin is degraded; or that the α-sarcin may not enter the pathway from which CPV penetrates the endosomal membrane. The last hypothesis is supported by the observation that CPV did not colocalize with FITC-dextran (Fig. 7B), which like α-sarcin enters cells through fluid-phase endocytosis (29).

CPV particles colocalize with Tfn in endosomes. CPV particles clearly colocalized with Tfn in perinuclear vesicles of Mv1Lu-TR cells after 2 h at 37°C (Fig. 7A). As Tfn efficiently enters the perinuclear recycling vesicle in nonpolarized cells (84) and more than 80% of the cell TfnR molecules reside in this recycling compartment (34), it appears that CPV is also trafficked to and becomes retained in the perinuclear recycling vesicle. This would be consistent with the observation that CPV particles do not become degraded even after many hours of incubation with cells (83), as proteases are excluded from the perinuclear recycling endosomes, but they would normally be present in late endosomes or lysosomes.

We propose a model of cell entry events associated with CPV infection. CPV first binds to a receptor on the cell surface and then is rapidly transported by clathrin-mediated endocytosis into an early sorting endosome, where the virus is segregated from fluid-phase ligands and within 10 min is transported to perinuclear recycling vesicles. The virus may penetrate to the cytoplasm, allowing DNA delivery to the nucleus, either from this compartment or after further transport to another, as yet unidentified vesicular compartment. Our data would support the latter possibility, as the late effect of BFLA1 on infection suggests that virus may be transported to another vesicular compartment, perhaps the late endosome as suggested by Vihinen-Ranta et al. (81). We are further testing this proposed model in our current studies.

ACKNOWLEDGMENTS

Electron microscopy was provided by the Cornell Integrated Microscopy Center. Wendy Weichert and Gail Sullivan provided expert technical assistance.

This work was supported by grants AI28385 and AI33468 to C.R.P. from the National Institutes of Health. J.S.L.P. was supported by a graduate research assistantship from the College of Veterinary Medicine at Cornell and by National Research Service fellowship F32 AI10134.

REFERENCES

1. **Al-Hasani, H., C. S. Hinck, and S. W. Cushman.** 1998. Endocytosis of the glucose transporter GLUT4 is mediated by the GTPase dynamin. J. Biol. Chem. **273:**17504–17510.
2. **Anderson, H. A., Y. Chen, and L. C. Norkin.** 1996. Bound simian virus 40 translocates to caveolin-enriched membrane domains, and its entry is inhibited by drugs that selectively disrupt caveolae. Mol. Biol. Cell **7:**1825–1834.
3. **Anderson, R. G. W., B. A. Kamen, K. G. Rothberg, and S. W. Lacey.** 1992. Potocytosis: sequestration and transport of small molecules by caveolae. Science **255:**410–411.
4. **Authier, F., B. I. Posner, and J. J. Bergeron.** 1996. Endosomal proteolysis of internalized proteins. FEBS Lett. **389:**55–60.
5. **Barbis, D. P., S.-F. Chang, and C. R. Parrish.** 1992. Mutations adjacent to the dimple of the canine parvovirus capsid structure affect sialic acid binding. Virology **191:**301–308.
6. **Barbis, D. P., and C. R. Parrish.** 1994. Characterization of canine parvovirus (CPV) interactions with 3201 T cells: involvement of GPI-anchored protein(s) in binding and infection. Braz. J. Med. Biol. Res. **27:**401–407.
7. **Basak, S., and R. W. Compans.** 1989. Polarized entry of canine parvovirus in an epithelial cell line. J. Virol. **63:**3164–3167.
8. **Basak, S., and H. Turner.** 1992. Infectious entry pathway for canine parvovirus. Virology **186:**368–376.
9. **Basak, S., H. Turner, and S. Parr.** 1994. Identification of a 40- to 42-kDa attachment polypeptide for canine parvovirus in A72 cells. Virology **205:**7–16.
10. **Bayer, N., D. Schober, E. Prchla, R. F. Murphy, D. Blaas, and R. Fuchs.** 1998. Effect of bafilomycin A1 and nocodazole on endocytic transport in HeLa cells: implications for viral uncoating and infection. J. Virol. **72:**9645–9655.
11. **Bowman, E. J., A. Siebers, and K. Altendorf.** 1988. Bafilomycins: a class of inhibitors of membrane ATPases from microorganisms, animal cells, and plant cells. Proc. Natl. Acad. Sci. USA **85:**7972–7976.
12. **Brown, K. E., S. M. Anderson, and N. S. Young.** 1993. Erythrocyte P antigen: cellular receptor for B19 parvovirus. Science **262:**114–117.
13. **Bullough, P. A., F. M. Hughson, J. J. Skehel, and D. C. Wiley.** 1994. Structure of influenza haemagglutinin at the pH of membrane fusion. Nature **371:**37–43.
14. **Cao, H., F. Garcia, and M. A. McNiven.** 1998. Differential distribution of dynamin isoforms in mammalian cells. Mol. Biol. Cell **9:**2595–2609.
15. **Chang, S.-F., J.-Y. Sgro, and C. R. Parrish.** 1992. Multiple amino acids in the capsid structure of canine parvovirus coordinately determine the canine host range and specific antigenic and hemagglutination properties. J. Virol. **66:**6858–6867.
16. **Chen, M. S., R. A. Obar, C. C. Schroeder, T. W. Austin, C. A. Poodry, S. C. Wadsworth, and R. B. Vallee.** 1991. Multiple forms of dynamin are encoded by shibire, a Drosophila gene involved in endocytosis. Nature **351:**583–586.
17. **Clague, M. J., S. Urbe, F. Aniento, and J. Gruenberg.** 1994. Vacuolar ATPase activity is required for endosomal carrier vesicle formation. J. Biol. Chem. **269:**21–24.
18. **Clark, S. G., D. L. Shurland, E. M. Meyerowitz, C. I. Bargmann, and A. M. van der Bliek.** 1997. A dynamin GTPase mutation causes a rapid and reversible temperature-inducible locomotion defect in C. elegans. Proc. Natl. Acad. Sci. USA **94:**10438–10443.
19. **Cotmore, S. F., and P. Tattersall.** 1987. The autonomously replicating parvoviruses of vertebrates. Adv. Virus Res. **33:**91–174.
20. **Cotten, M., E. Wagner, K. Zatloukal, and M. L. Birnstiel.** 1993. Chicken adenovirus (CELO virus) particles augment receptor-mediated DNA delivery to mammalian cells and yield exceptional levels of stable transformants. J. Virol. **67:**3777–3785.
21. **Cotten, M., E. Wagner, K. Zatloukal, S. Phillips, D. T. Curiel, and M. L. Birnstiel.** 1992. High-efficiency receptor-mediated delivery of small and large (48 kilobase gene constructs using the endosome-disruption activity of defective or chemically inactivated adenovirus particles. Proc. Natl. Acad. Sci. USA **89:**6094–6098.
22. **Cuadras, M. A., C. F. Arias, and S. Lopez.** 1997. Rotaviruses induce an early membrane permeabilization of MA104 cells and do not require a low intracellular Ca^{2+} concentration to initiate their replication cycle. J. Virol. **71:**9065–9074.
23. **Damke, H.** 1996. Dynamin and receptor-mediated endocytosis. FEBS Lett. **389:**48–51.
24. **Damke, H., T. Baba, A. M. van der Bliek, and S. L. Schmid.** 1995. Clathrin-independent pinocytosis is induced in cells overexpressing a temperature-sensitive mutant of dynamin. J. Cell Biol. **131:**69–80.
25. **Damke, H., T. Baba, D. E. Warnock, and S. L. Schmid.** 1994. Induction of mutant dynamin specifically blocks endocytic coated vesicle formation. J. Cell Biol. **127:**915–934.
26. **Damke, H., M. Gossen, S. Freundlieb, H. Bujard, and S. L. Schmid.** 1995. Tightly regulated and inducible expression of dominant interfering dynamin mutant in stably transformed HeLa cells. Methods Enzymol. **257:**209–220.
27. **DeTulleo, L., and T. Kirchhausen.** 1998. The clathrin endocytic pathway in viral infection. EMBO J. **17:**4585–4593.
28. **Doms, R. W., A. Helenius, and J. White.** 1985. Membrane fusion activity of

the influenza virus hemagglutinin. The low pH-induced conformational change. J. Biol. Chem. **260:**2973–2981.
29. **Fernandez-Puentes, C., and L. Carrasco.** 1980. Viral infection permeabilizes mammalian cells to protein toxins. Cell **20:**769–775.
30. **Fitzgerald, D. J. P., R. Padmanabhan, I. Pastan, and M. C. Willingham.** 1983. Adenovirus-induced release of epidermal growth factor and pseudomonas toxin into the cytosol of KB cells during receptor-mediated endocytosis. Cell **32:**607–617.
31. **Fox, J. M., and M. E. Bloom.** 1999. Identification of a cell surface protein from Crandell feline kidney cells that specifically binds Aleutian mink disease parvovirus. J. Virol. **73:**3835–3842.
32. **Gagnon, A. W., L. Kallal, and J. L. Benovic.** 1998. Role of clathrin-mediated endocytosis in agonist-induced down-regulation of the β2-adrenergic receptor. J. Biol. Chem. **273:**6976–6981.
33. **Gruenberg, J., G. Griffiths, and K. E. Howell.** 1989. Characterization of the early endosome and putative endocytic carrier vesicles in vivo and with an assay of vesicle fusion in vitro. J. Cell Biol. **108:**1301–1316.
34. **Gruenberg, J., and F. R. Maxfield.** 1995. Membrane transport in the endocytic pathway. Curr. Opin. Cell Biol. **7:**552–563.
35. **Guinea, R., and L. Carrasco.** 1995. Requirement for vacuolar proton-ATPase activity during entry of influenza virus into cells. J. Virol. **69:**2306–2312.
36. **Helenius, A., J. Kartenbeck, K. Simons, and E. Fries.** 1980. On the entry of Semliki forest virus into BHK-21 cells. J. Cell Biol. **84:**404–420.
37. **Henley, J. R., E. W. Krueger, B. J. Oswald, and M. A. McNiven.** 1998. Dynamin-mediated internalization of caveolae. J. Cell Biol. **141:**85–99.
38. **Horiuchi, M., N. Ishiguro, H. Goto, and M. Shinagawa.** 1992. Characterization of the stage(s) in the virus replication cycle at which the host-cell specificity of the feline parvovirus subgroup is regulated in canine cells. Virology **189:**600–608.
39. **Johnson, L. S., K. W. Dunn, B. Pytowski, and T. E. McGraw.** 1993. Endosome acidification and receptor trafficking: bafilomycin A1 slows receptor externalization by a mechanism involving the receptor's internalization motif. Mol. Biol. Cell **4:**1251–1266.
40. **Jones, S. M., K. E. Howell, J. R. Henley, H. Cao, and M. A. McNiven.** 1998. Role of dynamin in the formation of transport vesicles from the trans-Golgi network. Science **279:**573–577.
41. **Kaljot, K. T., R. D. Shaw, D. H. Rubin, and H. B. Greenberg.** 1988. Infectious rotavirus enters cells by direct cell membrane penetration, not by endocytosis. J. Virol. **62:**1136–1144.
42. **Kartenbeck, J., H. Stukenbrok, and A. Helenius.** 1989. Endocytosis of simian virus 40 into the endoplasmic reticulum. J. Cell Biol. **109:**2721–2729.
43. **Kielian, M.** 1995. Membrane fusion and the alphavirus life cycle. Adv. Virus Res. **45:**113–151.
44. **Kielian, M., and A. Helenius.** 1985. pH-induced alterations in the fusogenic spike protein of Semliki forest virus. J. Cell Biol. **101:**2284–2291.
45. **Laffin, J., and J. M. Lehman.** 1990. Detection of intracellular virus and viral products. Methods Cell Biol. **33:**271–284.
46. **Linser, P., H. Bruning, and R. W. Armentrout.** 1979. Uptake of minute virus of mice into cultured rodent cells. J. Virol. **31:**537–545.
47. **Luo, M., J. Tsao, M. G. Rossmann, S. Basak, and R. W. Compans.** 1988. Preliminary X-ray crystallographic analysis of canine parvovirus crystals. J. Mol. Biol. **200:**209–211.
48. **Maizel, J. V., D. O. White, and M. D. Scharff.** 1968. The polypeptides of adenovirus. I. Evidence for multiple protein components in the virion and a comparison of types 2, 7A, and 12. Virology **36:**115–125.
49. **Mallard, F., C. Antony, D. Tenza, J. Salamero, B. Goud, and L. Johannes.** 1998. Direct pathway from early/recycling endosomes to the Golgi apparatus revealed through the study of shiga toxin B-fragment transport. J. Cell Biol. **143:**973–990.
50. **Marsh, M., and A. Helenius.** 1989. Virus entry into animal cells. Adv. Virus Res. **36:**107–151.
51. **Marsh, M., and A. Pelchen-Matthews.** 1994. The endocytic pathway and virus entry, p. 215–240. *In* E. Wimmer (ed.), Cellular receptors for animal viruses, vol. 28. Cold Spring Harbor Laboratory Press, Cold Spring Harbor, N.Y.
52. **Martinez, C. G., R. Guinea, J. Benavente, and L. Carrasco.** 1996. The entry of reovirus into L cells is dependent on vacuolar proton-ATPase activity. J. Virol. **70:**576–579.
53. **Matlin, K. S., H. Reggio, A. Helenius, and K. Simons.** 1981. Infectious entry pathway of influenza virus in a canine kidney cell line. J. Cell Biol. **91:**601–613.
54. **Matlin, K. S., H. Reggio, A. Helenius, and K. Simons.** 1982. Pathway of vesicular stomatitis virus entry leading to infection. J. Mol. Biol. **156:**609–631.
55. **Mellman, I.** 1996. Endocytosis and molecular sorting. Annu. Rev. Cell Dev. Biol. **12:**575–625.
56. **Mizukami, H., N. S. Young, and K. E. Brown.** 1996. Adeno-associated virus type 2 binds to a 150-kilodalton cell membrane glycoprotein. Virology **217:**124–130.
57. **Nibert, M. L., and B. N. Fields.** 1994. Early steps in reovirus infection of cells, p. 341–364. *In* E. Wimmer (ed.), Cellular receptors for animal viruses, vol. 28. Cold Spring Harbor Laboratory Press, Cold Spring Harbor, N.Y.
58. **Parker, J. S. L., and C. R. Parrish.** 1997. Canine parvovirus host range is determined by the specific conformation of an additional region of the capsid. J. Virol. **71:**9214–9222.
59. **Parrish, C. R.** 1991. Mapping specific functions in the capsid structure of canine parvovirus and feline panleukopenia virus using infectious plasmid clones. Virology **183:**195–205.
60. **Patterson, S., and W. C. Russell.** 1983. Ultrastructural and immunofluorescence studies of early events in adenovirus-HeLa cell interactions. J. Gen. Virol. **64:**1091–1099.
61. **Perez, L., and L. Carrasco.** 1993. Entry of poliovirus into cells does not require a low-pH step. J. Virol. **67:**4543–4548.
62. **Perez, L., and L. Carrasco.** 1994. Involvement of the vacuolar H(+)-ATPase in animal virus entry. J. Gen. Virol. **75:**2595–2606.
63. **Prchla, E., E. Kuechler, D. Blaas, and R. Fuchs.** 1994. Uncoating of human rhinovirus serotype 2 from late endosomes. J. Virol. **68:**3713–3723.
64. **Presley, J. F., S. Mayor, T. E. McGraw, K. W. Dunn, and F. R. Maxfield.** 1997. Bafilomycin A1 treatment retards transferrin receptor recycling more than bulk membrane recycling. J. Biol. Chem. **272:**13929–13936.
65. **Qing, K., C. Mah, J. Hansen, S. Zhou, V. Dwarki, and A. Srivastava.** 1999. Human fibroblast growth factor receptor 1 is a co-receptor for infection by adeno-associated virus 2. Nat. Med. **5:**71–77.
66. **Ren, M., G. Xu, J. Zeng, C. De Lemos-Chiarandini, M. Adesnik, and D. D. Sabatini.** 1998. Hydrolysis of GTP on rab11 is required for the direct delivery of transferrin from the pericentriolar recycling compartment to the cell surface but not from sorting endosomes. Proc. Natl. Acad. Sci. USA **95:**6187–6192.
67. **Reynisdottir, I., K. Polyak, A. Iavarone, and J. Massague.** 1995. Kip/Cip and Ink4 Cdk inhibitors cooperate to induce cell cycle arrest in response to TGF-β. Genes Dev. **9:**1831–1845.
68. **Riezman, H., P. G. Woodman, G. van Meer, and M. Marsh.** 1997. Molecular mechanisms of endocytosis. Cell **91:**731–738.
69. **Rigg, R. J., and H. Schaller.** 1992. Duck hepatitis B virus infection of hepatocytes is not dependent on low pH. J. Virol. **66:**2829–2836.
70. **Sodeik, B., M. W. Ebersold, and A. Helenius.** 1997. Microtubule-mediated transport of incoming herpes simplex virus 1 capsids to the nucleus. J. Cell Biol. **136:**1007–1021.
71. **Strassheim, M. L., A. Gruenberg, P. Veijalainen, J.-Y. Sgro, and C. R. Parrish.** 1994. Two dominant neutralizing antigenic determinants of canine parvovirus are found on the threefold spike of the virus capsid. Virology **198:**175–184.
72. **Summerford, C., J. S. Bartlett, and R. J. Samulski.** 1999. αVβ5 integrin: a co-receptor for adeno-associated virus type 2 infection. Nat. Med. **5:**78–82.
73. **Summerford, C., and R. J. Samulski.** 1998. Membrane-associated heparan sulfate proteoglycan is a receptor for adeno-associated virus type 2 virions. J. Virol. **72:**1438–1445.
74. **Suomalainen, M., M. Y. Nakano, S. Keller, K. Boucke, R. P. Stidwill, and U. F. Greber.** 1999. Microtubule-dependent plus- and minus end-directed motilities are competing processes for nuclear targeting of adenovirus. J. Cell Biol. **144:**657–672.
75. **Tosteson, M. T., and M. Chow.** 1997. Characterization of the ion channels formed by poliovirus in planar lipid membranes. J. Virol. **71:**507–511.
76. **Truyen, U., and C. R. Parrish.** 1995. The evolution and control of parvovirus host ranges. Semin. Virol. **6:**311–317.
77. **Urrutia, R., J. R. Henley, T. Cook, and M. A. McNiven.** 1997. The dynamins: redundant or distinct functions for an expanding family of related GTPases? Proc. Natl. Acad. Sci. USA **94:**377–384.
78. **van der Bliek, A. M., and E. M. Meyerowitz.** 1991. Dynamin-like protein encoded by the Drosophila shibire gene associated with vesicular traffic. Nature **351:**411–414.
79. **Varga, M. J., C. Weibull, and E. Everitt.** 1991. Infectious entry pathway of adenovirus type 2. J. Virol. **65:**6061–6070.
80. **Vieira, A. V., C. Lamaze, and S. L. Schmid.** 1996. Control of EGF-receptor signalling by clathrin-mediated endocytosis. Science **274:**2086–2089.
81. **Vihinen-Ranta, M., A. Kalela, P. Makinen, L. Kakkola, V. Marjomaki, and M. Vuento.** 1998. Intracellular route of canine parvovirus entry. J. Virol. **72:**802–806.
82. **Wang, K., S. Huang, A. Kapoor-Munshi, and G. Nemerow.** 1998. Adenovirus internalization and infection require dynamin. J. Virol. **72:**3455–3458.
83. **Weichert, W. S., J. S. L. Parker, A. T. M. Wahid, S. F. Chang, E. Meier, and C. R. Parrish.** 1998. Assaying for structural variation in the parvovirus capsid and its role in infection. Virology **250:**106–117.
84. **Yamashiro, D. J., B. Tycko, S. R. Fluss, and F. R. Maxfield.** 1984. Segregation of transferrin to a mildly acidic (pH 6.5) para-Golgi compartment in the recycling pathway. Cell **37:**789–800.
85. **Yeung, D. E., G. W. Brown, P. Tam, R. H. Russnak, G. Wilson, I. Clark-Lewis, and C. R. Astell.** 1991. Monoclonal antibodies to the major nonstructural nuclear protein of minute virus of mice. Virology **181:**35–45.
86. **Yu, R., and P. M. Hinkle.** 1998. Signal transduction, desensitization, and recovery of responses to thyrotropin-releasing hormone after inhibition of receptor internalization. Mol. Endocrinol. **12:**737–749.